Desalination and Water Treatment
www.deswater.com

doi: 10.5004/dwt.2022.28128

248 (2022) 268–276
February

Modification of glassy carbon surface using L-cysteine-capped Mn-doped ZnS quantum dots and multi wall carbon nanotube nanocomposite: application to determine hydrazine in water samples

Nader Amini[a,*], Mohammad Bagher Gholivand[b], Mojtaba Shamsipur[b,*], Afshin Maleki[a], Kazhal Naderi[c], Nader Marzban[d], Seung-Mok Lee[e], Choong Jeon[f,*]

[a]*Environmental Health Research Center, Research Institute for Health Development, Kurdistan University of Medical Sciences, Sanandaj, Iran, Tel. +98-21-66809032; email: naderamini95@yahoo.com (N. Amini), Maleki43@yahoo.com (A. Maleki)*
[b]*Department of Analytical Chemistry, Razi University, Kermanshah, Iran, Tel. +98-21-66908030; emails: mshamsipur@yahoo.com (M. Shamsipur), mbgholivand@yahoo.com (M.B. Gholivand)*
[c]*Vice Chancellor for Food & Drugs Administration, Kurdistan University of Medical Sciences, Sanandaj, Iran, email: na_kazhal84@yahoo.com (K. Naderi)*
[d]*Leibniz Institute for Agricultural Engineering and Bioeconomy, Max-Eyth-Allee 100, 14469 Potsdam-Bornim, Germany, email: Nader.marzban89@gmail.com (N. Marzban)*
[e]*Department of Environmental Engineering, Catholic Kwandong University, Gangneung 25601, South Korea, email: leesm@cku.ac.kr (S.-M. Lee)*
[f]*Department of Biochemical Engineering, Gangneung-Wonju National University, Gangneung 25457, South Korea, Tel. +82-33-640-2405; email: metaljeon@gwnu.ac.kr (C. Jeon)*

Received 27 June 2021; Accepted 28 December 2021

ABSTRACT

Mn-ZnS QDs synthesized by hydrothermal method and modified by L-cysteine for better stability emit phosphorescence at 590 nm. The characterization of L-cysteine-capped Mn-Doped ZnS quantum dots were studied by transmission electron microscopy (TEM), phosphorescence, fluorimetry and UV-Vis absorption spectroscopy. To fabricate a new electrochemical sensor, L-cysteine-capped Mn-Doped ZnS quantum dots and multiwall carbon nanotube (MWCNT) were placed on the surface of glassy carbon electrode (ZnS/MnQDs-MWCNTs/GCE). Then, it was applied for the determination and detection of environmental pollutant hydrazine in water samples. The electrooxidation behaviors and the effective stepwise assembly procedure of the modified electrode were confirmed by electrochemical impedance spectroscopy (EIS), scanning electron microscopy (SEM), cyclic voltammetry (CV) and differential pulse voltammetry (DPV). Based on the findings, ZnS/Mn QDs-MWCNT composite can be considered a suitable candidate for hydrazine electrooxidation. The linear rang, detection of limit (DL), limit of quantification (LOQ) and sensitivity were 90–1,200 nanomolar, 28 nM, 95 nM and 0.001 μA nM^{-1}, respectively. The repeatability in the presence of hydrazine (100 μM) was studied and the variation coefficient (R.S.D) was 2% for five consecutive tests. The proposed sensor shows many advantages such as very low detection of limit, high sensitivity, stability and it can be used for detection of hydrazine in real samples.

Keywords: Hydrazine; ZnS/Mn quantum dots; Multi wall carbon nanotube; Pollutant

* Corresponding authors.

1944-3994/1944-3986 © 2022 Desalination Publications. All rights reserved.

1. Introduction

Hydrazine (N_2H_4) has many uses in the aerospace, industrial, military and pharmacological fields. N_2H_4 is widely applied as antioxidant, catalyst, emulsifier, pesticide, corrosion inhibitor, deoxidizers in boilers reducing agent and in photo printing and pharmaceuticals. Moreover, it is used in fuel cells, military and aerospace industries, high-energy propellants in rockets and weapons for mass destruction. Hydrazine is a neurotoxin and it can affect kidneys, lungs and liver as well as cause respiratory tract infections. It also produces carcinogenic and mutagenic effects. Accordingly, finding a sensitive and appropriate analytical method for the determination and detection of hydrazine is essential [1]. For the determination of hydrazine, the following methods have been reported: spectrophotometry [2] electrochemical [3] titration [4] luminescence [5] flow injection analysis [6,7] and chromatography [8]. Amongst the aforementioned methods, the electrochemical method is sensitive, rapid, selective, low cost and effective. However, in this method, direct oxidation is not possible or requires a large over potential with conventional electrodes. Hydrazine is oxidized at high potential and its direct oxidation is not possible with conventional electrodes which limits the application of electrochemical methods for detecting and determining N_2H_4. The electrochemical treatment in regard to some materials, including N_2H_4, depends on the structure of the electrode surface [9]. Direct hydrazine oxidation at several electrode surfaces such as gold, silver, mercury [10], platinum [11], nickel [12] and rhodium [9] have been reported. For minimizing over-potential and enhancing the electron transfer rate, the surface of the electrode should be modified. Several modifiers such as hematoxylin [13], chlorogenic acid [14,15], acetylferrocene [16], coumestan [17], 4-pyridyl hydroquinone [18,19], metals [20–22], CdSe quantum dots @ nickel hexacyanoferrate core–shell nanoparticles [q1] and Carbon Quantum Dots [q2] are applied to minimize over potential and increase charge-transfer rate [25].

Carbon nanotubes (CNT) have unique chemical, electrical, thermal, optical and mechanical properties in addition to a particularly large surface area. For this reason, they have been applied in microelectronics, environment, composite materials, biosensors, modifiers of electrode surfaces and particularly in the field of environmental monitoring and sensing [26,27]. The materials of carbon nanotube as composite can further enhance an electrode's electrocatalytic capability as exemplified in metal blue/CNT composite for oxidizing nicotinamide adenine dinucleotide and ZnONps/MWCNT/chitosan modifier for detecting the sequence-specific of PAT genes. The use of nanometer-sized conducting and semiconducting materials such as quantum dots (QDs) has attracted significant attention in research studies [28]. Quantum dots, semiconductor crystals are 1 to 10 nanometers in diameter. These materials contain group II–VI elements or group III–V elements. Because these materials are size-tunable and chemically functionalizable, and have catalytic effect properties, they are used as modifiers in electrochemical sensors and biosensors. For instance, Wang et al. presented a new electrochemical biosensor based on horseradish peroxidase (HPR) and liophilic Cd/ZnS QDs for detection of H_2O_2 [29]. Liu et al. [30] reported an innovative electrochemical biosensor by modifying a glassy carbon electrode with glucose oxidase/CNT/CdTe QDs nanocomposite for glucose samples. In addition, the electrochemical behaviors of hemoglobin and glucose oxidase were and investigated [21–32]. Recently, a novel class of quantum dots (doped quantum dots, d-dots) found on transition-metal-ion-doped QDs in the absence of heavy-metal ions (cadmium, mercury as well as lead) was studied. These compounds have unique properties such as photostability, temperature stability, zero-reabsorption, low cytotoxicity and highly emissive d-dots as efficient as standard QDs which have been considered for the manufacture of sensors and biosensors. Manganese is suitable under industrial standards as exemplified in studies investigating ZnSe and ZnS doped with Mn ions [33]. In this study, the application of ZnS/Mn QDs-MWCNTs as a mediator for electrooxidation of hydrazine at pH = 7 was investigated. Due to stability, very low detection of limit, simple preparation and antifouling properties, ZnS/Mn QDs-MWCNTs/GCE was used as an amperometric sensor for nanomolar detection of hydrazine.

2. Experimental

2.1. Reagents

L-cysteine amino acid, hydrazine, manganese chloride ($MnCl_2$), zinc sulfate ($ZnSO_4$), and sodium sulfide (Na_2S) were obtained from Merck Company, and MWCNT from Sigma-Aldrich. In addition, (Na_3PO_4), (Na_2HPO_4), (NaH_2PO_4), (HCl) and (NaOH) materials were used for buffer preparation.

2.2. Instruments

Electrochemical tests were conducted with a computer controlling μ-system (Eco ChemieU/techt). Electrochemical analysis was carried out by a platinum counter, a glassy carbon (GC) as a working and Ag/AgCl [KCl (sat)] as a reference electrode. These electrodes were obtained from Metrohm Company.

2.3. Preparation synthesis of ZnS/Mn quantum dots

Preparation of L-cysteine-capped Mn-Doped ZnS quantum dots was performed based on the reported procedures [34,35]. A typical synthesis procedure is as follows. 4 mL of 0.1 molar zinc sulfate and 50 mL of L-cys amino acid (0.02 M) were transferred into a three-necked flask. The pH of the solution was then adjusted to 11 using sodium hydroxide and purged with pure N_2 gas for 40 min under magnetic stirring. Subsequently, 4 mL of 0.01 M manganese(II) chloride was added into the prepared solution and stirred again for 40 min. Then, 5 mL of 0.1 molar Na_2S was added to the vortex of solution and was stirred for 70 min. This was followed by the solution being sealed and incubated for 12 h in 50°C water bath. Finally, it was centrifuged and washed with ethanol.

2.4. Fabrication of the modified electrode

First, the bare GCE was polished using emery papers and aluminum oxide slurry. In order to remove adsorbed

particles, this electrode was sonicated in distillate water and ethyl alcohol for 5 min. Then, 2 mg ZnS/Mn quantum dots and 1 mg multiwall carbon nanotube to stabilize the nanoparticles on the electrode surface (were added to 5 mL ethyl alcohol and ultra-sonicated for 40 min in order to prepare a homogeneous ZnS/Mn quantum dot-MWCNT solution. Finally, 6 μL of prepared solution was placed onto the bare GCE electrode and dried at room temperature.

3. Results and discussion

3.1. Characterization of ZnS/Mn quantum dots

As shown in Fig. 1A, UV-Vis absorption spectroscopy (a), fluorimetery (b) and phosphorescence (c) are used to examine the characteristics of Mn-doped ZnS QDs. According to Fig. 1A-a Mn-doped ZnS QDs has an absorption spectrum presenting a shoulder absorption peak at 282 nm, while ZnS nanoparticles has an absorption spectrum of 290 nm and a blue shift can be seen. These results are consistent with previous data [36]. The fluorescence behavior of ZnS QDs and Mn:ZnS QD's are demonstrated in Fig. 1B-b. As illustrated from the spectra, when the manganese ion is added, the red shift from 450 (ZnSQDs) to 600 nm (Mn:ZnS QDs) is seen. In Fig. 1Ac the phosphorescence behavior of Mn/ZnS QDs are presented. The phosphorescence emission spectrum of Mn:ZnS QDs depicting a symmetric profile peaked at 590 nm. The intense phosphorescence was associated with the transition of $(^4T_1) \rightarrow (^6A_1)$ for Mn^{2+} [37]. The morphology of the Mn-doped ZnS QDs was investigated by TEM. The results suggested that the Mn-doped ZnS QDs are almost spherical, with an average particle diameter of 9 nm (Fig. 1B).

Based on the XRD pattern (Fig. 2A), it can be observed that three broad peaks related to (311), (220), and (111) reflecting planes prove Mn:ZnS dots to have a cubic zinc blende structure similar to un-doped ZnS quantum dots. Dopant manganese (II) did not affect the crystal structure of ZnS quantum dots. Based on the FT-IR spectra of Mn-ZnS QDs (Fig. 2B), the absorption peak at 3,466 cm^{-1} was related to the stretching vibration of hydroxyl groups in the carboxyl functional group and two absorption peaks at 3,330 and 3,270 cm^{-1} subjected to amino characteristics. Clearly, the N–C stretching peaked at 1,600 cm^{-1} and the absorption peak at 1,125 cm^{-1} was related to the carbonyl group in the carboxyl group. At 2,600 cm^{-1}, the mercapto vibrational peak disappeared due to the binding of the sulfhydryl and the surface of Mn-ZnS QDs.

3.2. Electrochemical characterization and morphological of ZnS/Mn QDs-MWCNTs/GC electrode

Fig. 3 indicates the SEM images of MWCNTs as well as ZnS/Mn QDs-MWCNTs directly placed on the surface of GCE as a uniformly distributed ZnS/Mn QDs in MWCNTs. In order to appraise the electrochemical efficacy of the electrodes and the changes in their surfaces, electrochemical impedance spectroscopy was applied. Fig. 4 indicates the Nyquist plots for several electrodes: bare GCE (a), MWCNT/GCE (b) and ZnS/Mn QDs/MWCNTs/GCE (c) in 5 mM $Fe(CN)_6^{3-/4-}$ probe. Based on the Nyquist plots, the semicircle section is related to charge transfer limited process and the diameter is related to the charge transfer. R_{ct} (charge transfer resistance), R_s (solution resistance), and C (the double layer capacitance) are presented in Fig. 4 (Inset) and the EIS data was obtained from the tested electrodes fitted on a simple equal circuit. In addition, a number of parameters were applied to fit the experimental electrochemical impedance results as shown in Table 1. Based on the results, for the bare GC electrode, the R_{ct} value was considerably high. When the MWCNT was employed, the R_{ct} value was decreased due to the increased charge transfer. When ZnS:Mn was added into the MWCNT composite, the R_{ct} value decreased substantially. This demonstrates the modification of the surface electrode and easier charge transfer between the electrode surface and the probe.

3.3. Electrocatalytic oxidation of N_2H_4 on ZnS/Mn QDs-MWCNTs/GCE

Through cyclic voltammetry technique, the electrocatalytic oxidation properties of ZnS/Mn QDs-MWCNTs/GCE was studied for analysis of the N_2H_4 sample. The results suggest that at the surfaces of GC and MWCNT/GC electrodes, no redox peak of hydrazine could be observed

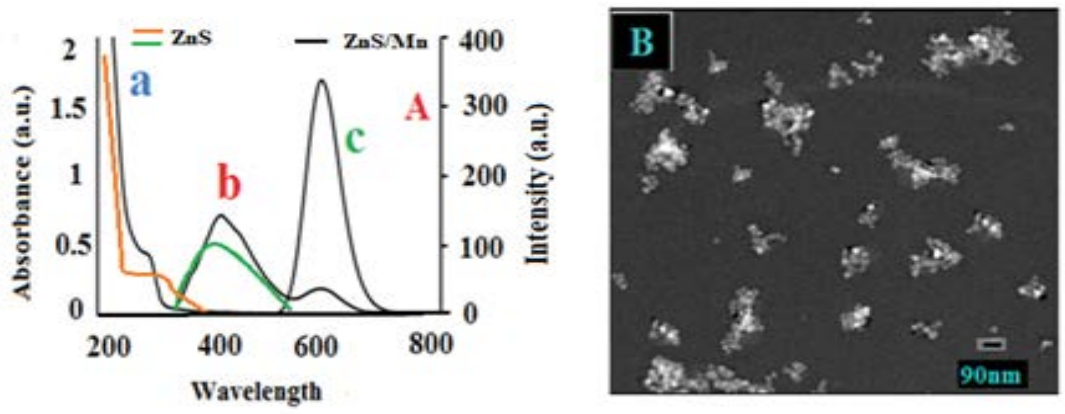

Fig. 1. (A) UV-Vis absorption (a), fluorescence emission (b) and room temperature phosphorescence (c) spectra of Mn-doped ZnS QDs. (B) Transmission electron microscopy image of Mn-doped ZnS QDs.

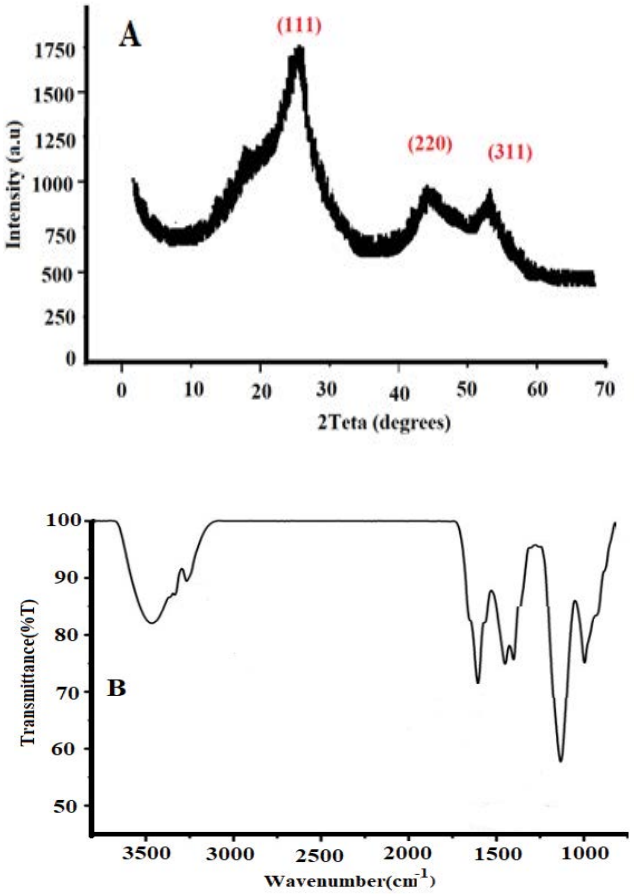

Fig. 2. XRD (A) and FTIR of Mn-doped ZnS QDs (B).

in the potential range of 0–1 V. However, at the ZnS/Mn QDs-MWCNTs/GCE surface, the anodic peaks current increased with catalytic oxidation of hydrazine as shown in Fig. 5. A substantial growth of peak current was observed denoting considerable catalytic capability of ZnS/Mn QDs-MWCNTs for hydrazine oxidation. Moreover, at the surface of ZnS/Mn QDs-MWCNTs/GCE, the overvoltage for hydrazine oxidation declined dramatically. Therefore, ZnS/Mn QDs-MWCNTs is a good mediator to shuttle electron between hydrazine sample and modified working electrode. For the purposes of investigating the electrocatalytic behavior and optimal pH of ZnS/Mn QDs-MWCNTs, the impact of pH on the electro-oxidation response of the ZnS/Mn QDs-MWCNTs/GCE to hydrazine was evaluated. The cyclic voltammograms (CVs) of the novel sensor in 180 μM hydrazine was investigated at different pH values. Based on Fig. 6, at pH range 2–9, the ZnS/Mn QDs-MWCNTs/GCE showed electrocatalytic behavior. However, the highest peak current was observed at pH 7. Furthermore, the electrochemical behavior of the proposed electrode in the presence of different amounts of hydrazine sample was investigated through the CV technique. Fig. 7 illustrates that the oxidation peak currents of the catalytic anodic peak at 0.4 V is increased linearly with increasing amounts of hydrazine sample. Based on the aforementioned results, a possible 4-electron process mechanism can be proposed, leading finally to the generation of nitrogen gas [Eqs. (1)–(3)]:

$$N_2H_4 + H_2O \rightarrow N_2H_3 + H_3O^+ + e^- \quad (1)$$

$$N_2H_3 + 3H_2O \rightarrow N_2 + 3H_3O^+ + 3e^- \quad (2)$$

$$N_2H_4 + 4H_2O \rightleftharpoons N_2 + 4H_3O^+ + 4e^- \text{ (Overall reaction)} \quad (3)$$

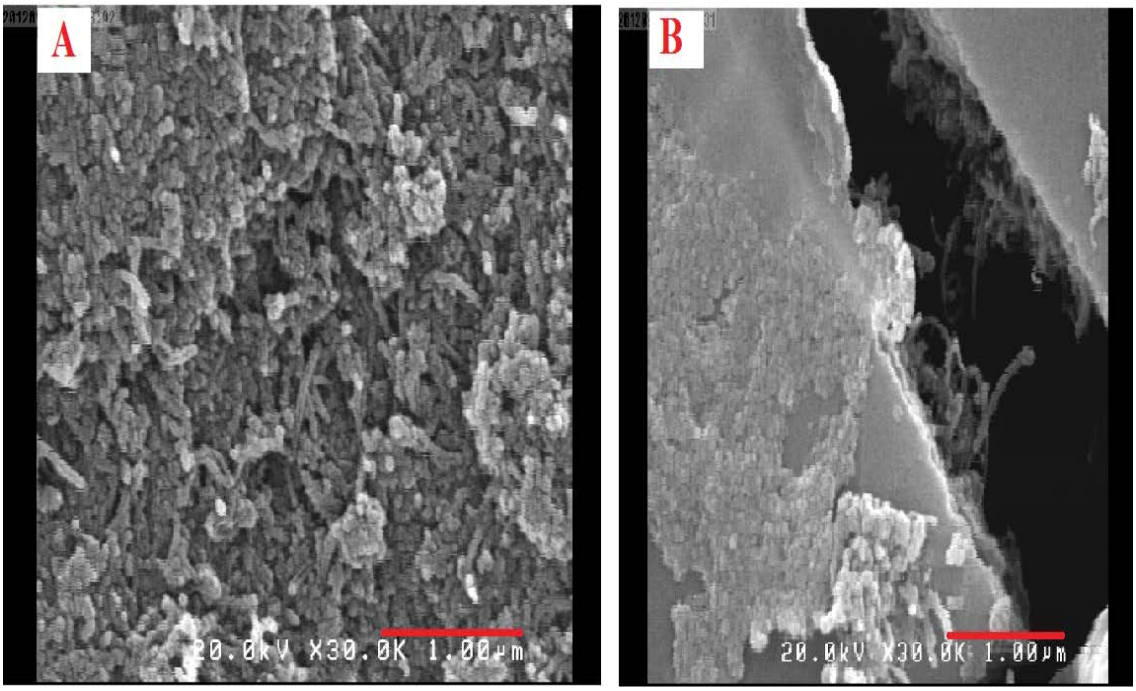

Fig. 3. SEM of MWCNT (A) and Mn-doped ZnS QDs/MWCNT (B).

Based on Fig. 7 (inset), the curves of anodic peak current vs. different amounts of hydrazine present a linear behavior from 10 to 200 μM. The sensitivity was calculated at approximately 0.0119 μA μM^{-1}. In addition, other parameters such as detection limit of 3 μM and the determination limit of 25.3 μM were obtained resulting in the proposed electrode possessing the capability for the detection and determination of hydrazine. Fig. 8 indicates the cyclic voltammograms of 100 μM of hydrazine sample at different potential scan rates (10–100 mV s^{-1}). The anodic peak currents for electrooxidation of hydrazine are proportional to the square root of the scan rate ($v^{1/2}$) (Fig. 8, inset), suggesting that the mechanism is under the control of diffusion. For obtaining the low detection limit, differential pulse voltammetry (DPV) is a good method. The differential pulse voltammograms of the proposed sensor in the presence of different amounts of hydrazine, 90–1,200 nM, are presented in Fig. 9. A linear relationship of the anodic peak currents (I_{pa}) vs. concentration of hydrazine can be presented in the I (μA) = 0.001 [hydrazine] μA nM^{-1} + 0.4607 μA equation. The detection of limit (DL) was 28 nM at S/N = 3.

3.4. Repeatability and stability

For the proposed electrode, the repeatability in the presence of hydrazine (100 μM) was studied and the variation coefficient (R.S.D) was 2% for five consecutive tests. The nanosensor's lifespan and stability were considered by investigating the response oxidation currents of the proposed nanosensor at time spans of 7 and 28 d. The decline in the electrode behaviors were 97% and 88.5% of initial oxidation current response after 7 and 28 d, respectively.

3.5. Interference effects

With the purpose of investigating the selectivity of the ZnS/Mn QDs-MWCNTs/GCE, the influence of some inorganic ions and phenolic compounds were studied in a buffer phosphate (pH = 7) containing 50 μM N_2H_4. Based on the results, 2-fold amounts of nitrophenol, phenol and a set of anions and cations for 20-fold amounts of F^-, Mg^{2+}, PO_4^{3-}, Br^-, Na^+, Li^+, Ca^{2+}, Cl^-, IO_3^-, $Pb^{2+}$and Zn^{2+} had no effects on N_2H_4 analysis.

3.6. Comparison of ZnS/Mn QDs-MWCNTs modified electrode with those of preceding electrodes

Table 2 compares the limit of detection, sensitivity and applied potential of the ZnS/Mn QDs-MWCNTs modified electrode for hydrazine determination with those of other hydrazine electrodes presented in previous reports, and

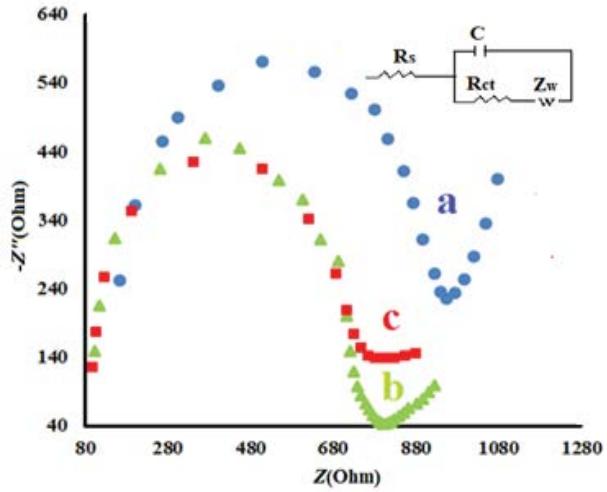

Fig. 4. Electrochemical impedance spectroscopy (EIS) of GCE (a) MWCNT/GCE, (b) Mn-doped ZnS QDs/MWCNT/GCE and (c) in 5 mM probe $Fe(CN)_6^{4/3-}$.

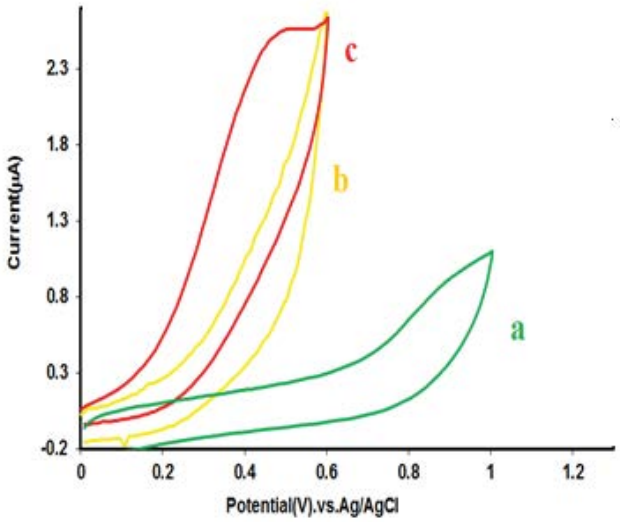

Fig. 5. Cyclic voltammograms of different electrodes: (a) unmodified, (b) MWCNT/GCE, (c) Mn-doped ZnS QDs/MWCNT/GCE in the presence of hydrazine.

Table 1
Electrochemical impedance spectroscopy data for different electrodes

R1(C[R2W])	GCE		GCE/MWCNT		GCE/MWCNT/ZnS:Mn	
	Value	Error (%)	Value	Error (%)	Value	Error (%)
R1	0.431 KΩ	3.028	398.5 Ω	5.409	389 KΩ	3.279
C	0.414 μF	6.782	0.432 μF	6.239	0.440 μF	3.153
R2	0.95 KΩ	3.324	0.84 KΩ	5.176	0.715 KΩ	3.222
W	0.3204×10^{-3}	10.291	0.20×10^{-3}	10.066	0.189×10^{-3}	5.14

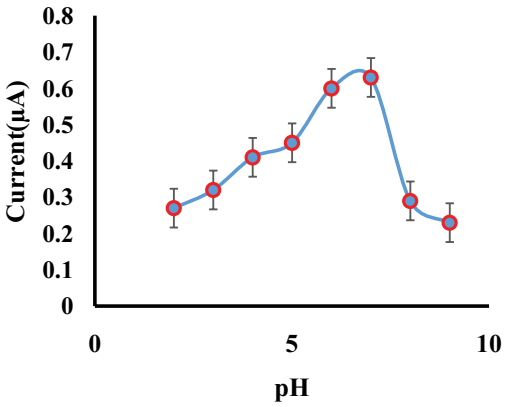

Fig. 6. The plot of a GCE modified for values pH (from 2 to 9).

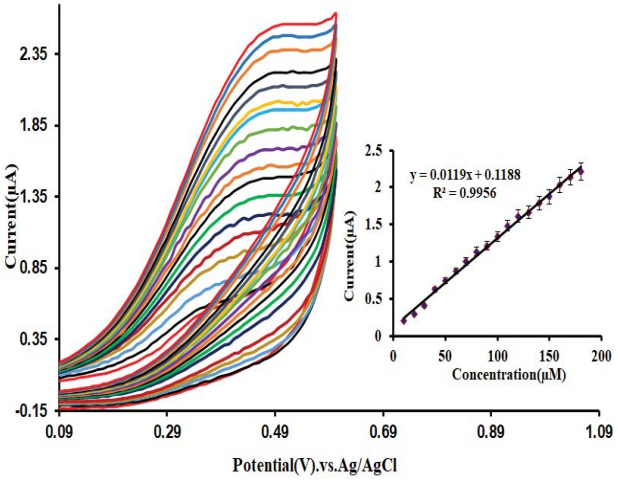

Fig. 7. Cyclic voltammograms of Mn-doped ZnS QDs/MWCNT/GCE in the presence of different concentrations of hydrazine from 10 and 180 μM. Inset, plot of I_p vs. hydrazine amounts.

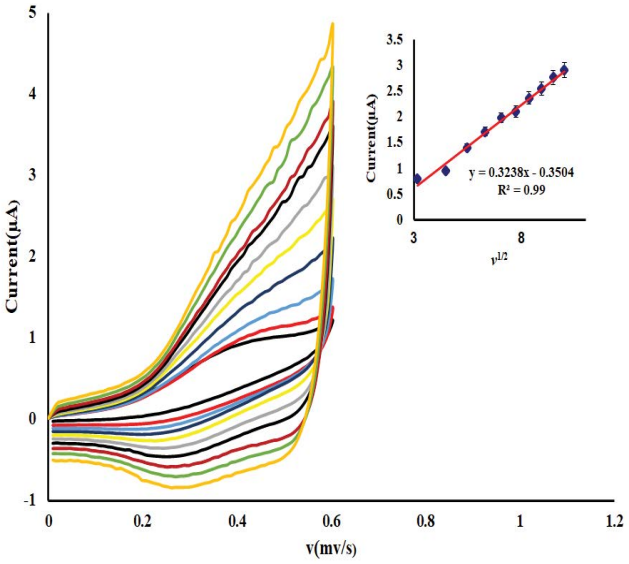

Fig. 8. Cyclic voltammetry curves of a Mn-doped ZnS QDs/MWCNT/GCE in the presence of hydrazine at different scan rates. Inset, plot of I_p vs. $v^{1/2}$.

demonstrates that the proposed electrode assays present a comparable or better properties for N_2H_4 detection.

3.7. Application

To evaluate the performance of ZnS/Mn QDs-MWCNTs modified electrode in practical applications, measurement of hydrazine in real matrix samples were investigated via a recovery parameter. As demonstrated in Table 3, the recoveries obtained (from 98.4 to 104.5) in measurement of hydrazine in different water samples (tap, mineral and lake waters) are satisfactory and ZnS/Mn QDs-MWCNTs/GCE is able to determine the concentration of hydrazine in water samples.

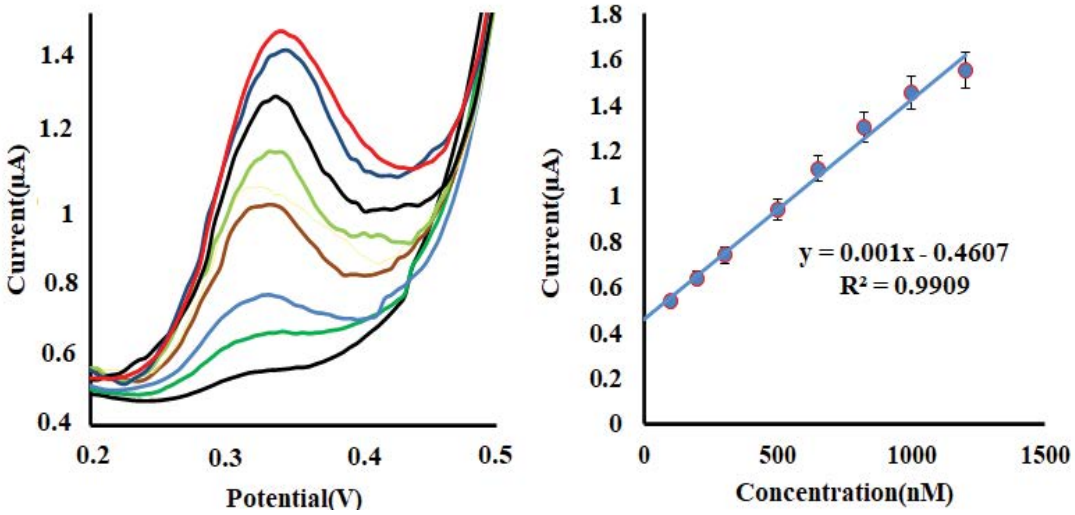

Fig. 9. DPV of Mn-doped ZnS QDs/MWCNT modified GC electrode in the presence of different concentrations of hydrazine from 100 to 1,200 nM. Inset, the curve of oxidation peak currents vs. hydrazine concentrations.

Table 2
Analytical parameters of several modified electrodes for determination of hydrazine

Electrode	pH	LOD	Dynamic rang	References
Ruthenium modified/GCE	5	8.5 μM	1,000–2,500 nM	[38]
Hexacyanoferrate modifiedgraphite–wax composite	7	6.65 μM	30–8,000 μM	[3]
Curcumin multi-wall carbon nanotubes modified/GCE	8	1.4 μM	2–44 μM	[39]
Nano-Au deposited on Porous-TiO_2 film	7	0.5 μM	2.50–500 μM	[40]
Pd/CILE	7	0.82 μM	5–800 μM	[41]
SPE/Cu–Pd	7.4	0.27 μM	2–100 μM	[42]
Pd/CNF-GCE	8.5	2.9 μM	10–4,000 μM	[43]
Pd nanoparticle modified BDD	7	6 μM	20–850 μM	[44]
Pd decorated bamboo MWCNTs	7	10 μM	56–157 μM	[45]
PANI/SrTiO3/GCE	7.2	1.09 μM	200–3,560 μM	[46]
MoS_2/Au/CM/PGE	7.4	18.3 nM	20–1,200 mM	[47]
PAMT-PGE	0.1 M KCl	–	1,500–16.740 × 10^4 μM	[48]
Cu_2O/MPC-2	NaOH	0.0358 μM	0.1–1,221 μM	[49]
ZnS/Mn quantum dots and multi-walled carbon nanotube/GCE	7	28 nM	90–1,200 nM	This work

Table 3
Determination of hydrazine content in water samples

Type of water	Added (μM)	Found (μM)[d]	RSD (%)[e]	Recovery (%)
Tap[a]	20	19.68	3.65	98.4
Mineral[b]	30	29.14	3.78	97.1
Lake[c]	20	20.91	4.21	104.5

[a]Water samples were collected from Kermanshah, Iran.
[b]Water samples were collected from Kimia Company, Kurdistan (Saghez), Iran.
[c]Water samples were collected from Sepide Kooh, Kurdistan (Saghez), Iran.
[d]Mean of four measurements.
[e]Relative standard deviation for $n = 4$.

4. Conclusions

In conclusion, authors reported a novel electrochemical sensor for sensitive detection of hydrazine. Firstly, Mn-Doped ZnS quantum dots (QDs) were obtained by hydrothermal technique and immobilized with multi wall carbon nanotube (MWCNT) on the surface of GC electrode. ZnS/Mn QDs and multi wall carbon nanotube (MWCNT) demonstrated excellent electrocatalytic properties for electrooxidation of N_2H_4 and the proposed electrode displayed advantages in some electrochemical parameters reported in research. The proposed method can be applied to other quantum dots and is recommended for the measurement of other samples.

References

[1] A. Umar, M.M. Rahman, Y.-B. Hahn, Ultra-sensitive hydrazine chemical sensor based on high-aspect-ratio ZnO nanowires, Talanta, 77 (2009) 1376–1380.
[2] A. Safavi, F. Abbasitabar, M.R. Hormozi Nezhad, Simultaneous kinetic spectrophotometric determination of isoniazid and hydrazine using H-point standard addition method, Chem. Anal. (Warsaw), 52 (2007) 835–845.
[3] D. Jayasri, S. Sriman Narayanan, Amperometric determination of hydrazine at manganese hexacyanoferrate modified graphite–wax composite electrode, J. Hazard. Mater., 144 (2007) 348–354.
[4] J.S. Budkuley, Mikrochim, Determination of hydrazine and sulfite in the presence of one another, Mikrochim. Acta, 108 (1992) 103–105.
[5] A. Safavi, M.A. Karimi, Flow injection chemiluminescence determination of hydrazine by oxidation with chlorinated isocyanurates, Talanta, 58 (2002) 785–792.
[6] J. Wang, Z. Lu, Electrocatalysis and determination of hydrazine compounds at glassy carbon electrodes coated with mixed-valent ruthenium (III, II) cyanide films, Electroanalysis, 1 (1989) 517–521.
[7] M. Ebadi, Electrocatalytic oxidation and flow amperometric detection of hydrazine on a dinuclear ruthenium phthalocyanine-modified electrode, Can. J. Chem., 81 (2003) 161–168.
[8] R. Gilbert, R. Rioux, Ion chromatographic determination of morpholine and cyclohexylamine in aqueous solutions containing ammonia and hydrazine, Anal. Chem., 56 (1984) 106–109.
[9] B. Alvarez-Ruiz, R. Gomez, J.M. Orts, J.M. Feliu, Role of the metal and surface structure in the electro-oxidation of hydrazine in acidic media, J. Electrochem. Soc., 149 (2002) D35–D45.
[10] K. Korinek, J. Koryta, M. Musilova, Electrooxidation of hydrazine on mercury, silver, and gold electrodes in alkaline solutions, J. Electroanal. Chem., 21 (1969) 319–327.
[11] M.D. Garcia-Azorero, M.L. Marcos, J.G. Velasco, Influence of changes in the total surface area and in the crystalline surface composition of Pt electrodes on their electrocatalytic properties

with respect to the electro-oxidation of hydrazine, Electrochim. Acta, 39 (1994) 1909–1914.
[12] M. Fleischmann, K. Korinek, D. Pletcher, Oxidation of hydrazine at a nickel anode in alkaline solution, J. Electroanal. Chem., 34 (1972) 499–503.
[13] H.R. Zare, N. Nasirizadeh, Hematoxylin multi-wall carbon nanotubes modified glassy carbon electrode for electrocatalytic oxidation of hydrazine, Electrochim. Acta, 52 (2007) 4153–4160.
[14] A. Salimi, R. Hallaj, Adsorption and reactivity of chlorogenic acid at a hydrophobic carbon ceramic composite electrode: application for the amperometric detection of hydrazine, Electroanalysis, 16 (2004) 1964–1971.
[15] A. Salimi, L. Miranzadeh, R. Hallaj, Amperometric and voltammetric detection of hydrazine using glassy carbon electrodes modified with carbon nanotubes and catechol derivatives, Talanta, 75 (2008) 147–156.
[16] R. Ojani, J.B. Raoof, B. Norouzi, Acetylferrocene modified carbon paste electrode; a sensor for electrocatalytic determination of hydrazine, Electroanalysis, 20 (2008) 1378–1382.
[17] H.R. Zare, N. Nasirizadeh, Electrocatalytic characteristics of hydrazine and hydroxylamine oxidation at coumestan modified carbon paste electrode, Electroanalysis, 18 (2006) 507–512.
[18] L. Niu, T.Y. You, J.Y. Gui, E.K. Wang, S.J. Dong, Electrocatalytic oxidation of hydrazines at a 4-pyridylhydroquinone self-assembled platinum electrode and its application to amperometric detection in capillary electrophoresis, J. Electroanal. Chem., 448 (1998) 79–86.
[19] T.Y. You, L. Niu, J.Y. Gui, S.J. Dong, E.K. Wang, Detection of hydrazine, methylhydrazine and isoniazid by capillary electrophoresis with a 4-pyridyl hydroquinone self-assembled microdisk platinum electrode, J. Pharm. Biomed. Anal., 19 (1999) 231–237.
[20] A. Abbaspour, M.A. Kamyabi, Electrocatalytic oxidation of hydrazine on a carbon paste electrode modified by hybrid hexacyanoferrates of copper and cobalt films, J. Electroanal. Chem., 576 (2005) 73–83.
[21] A. Salimi, K. Abdi, Enhancement of the analytical properties and catalytic activity of a nickel hexacyanoferrate modified carbon ceramic electrode prepared by two-step sol–gel technique: application to amperometric detection of hydrazine and hydroxyl amine, Talanta, 63 (2004) 475–483.
[22] H. Razmi, A. Azadbakht, M. Hsard, Application of a palladium hexacyanoferrate film-modified aluminum electrode to electrocatalytic oxidation of hydrazine, Anal. Sci., 21 (2005) 1317–1323.
[23] A. Kalaivani, S.S. Narayanan, Fabrication of CdSe quantum dots @ nickel hexacyanoferrate core–shell nanoparticles modified electrode for the electrocatalytic oxidation of hydrazine, J. Mater. Sci.: Mater. Electron., 29 (2018) 20146–20155.
[24] R. Sha, S.S. Jones, N. Vishnu, B. Soundiraraju, S. Badhulik, A novel biomass derived carbon quantum dots for highly sensitive and selective detection of hydrazine, Electroanalysis, 30 (2018) 1–6.
[25] S.K. Kim, Y.N. Jeong, M.S. Ahmad, J.M. You, H.C. Choi, S. Jeon, Electrocatalytic determination of hydrazine by a glassy carbon electrode modified with PEDOP/MWCNTs-Pd nanoparticles, Sens. Actuators, B, 153 (2011) 246–251.
[26] B. Song, M. Chen, S. Ye, P. Xu, G. Zeng, J. Gong, J. Li, P. Zhang, W. Cao, Effects of multi-walled carbon nanotubes on metabolic function of the microbial community in riverine sediment contaminated with phenanthrene, Carbon, 144 (2019) 1–7.
[27] B. Song, P. Xu, G. Zeng, J. Gong, P. Zhang, H. Feng, Y. Liu, X. Ren, Carbon nanotube-based environmental technologies: the adopted properties, primary mechanisms, and challenges, Rev. Environ. Sci. Biotechnol., 17 (2018) 571–590.
[28] L. Zheng, J.F. Song, Ni(II)-baicalein complex modified multi-wall carbon nanotube past electrode toward electrocatalytic oxidation of hydrazine, Talanta, 79 (2009) 319–326.
[29] Z. Wang, Q. Xu, H.Q. Wang, Q. Yang, J.H. Yu, Y.D. Zhaao, Hydrogen peroxide biosensor based on direct electron transfer of horseradish peroxidas with vapor deposited duantum dotes, Sens. Actuators, B, 138 (2009) 278–282.
[30] Q. Liu, X. Lu, J. Li, X. Yao, Direct electrochemistry of glucose oxidase and electrochemical biosensing of glucose on quantum dotes/carbon nanotubes electrodes, Biosens. Bioelectron., 22 (2007) 3203–3209.
[31] X.Y. Huang, W.J. Zhang, H. Xiao, G.X. Li, An electrochemical investigation of glucose oxidas at a CdS nanoparticles modified electrode, Biosens. Bioelectron., 21 (2005) 817–821.
[32] X.Y. Xu, J.G. Liang, C.G. Hu, F. Wang, S.H. Hu, Z.K. He, A hydrogen peroxide biosensor based on the direct electrochemistry of hemoglobin modified with quantum dotes, J. Biol. Inorg. Chem., 3 (2007) 421–427.
[33] J. Liu, X. Wei, Y. Qu, J. Cao, C. Chen, H, Jiang, Aqueous synthesis and bio-imaging application of highly luminescent and low cytotoxicity Mn^{2+}-doped ZnSe nanocrystals, Mater. Lett., 65 (2011) 2139–2141.
[34] Y. He, H.F. Wang, X.P. Yan, Exploring Mn-doped ZnS quantum dots for the room-temperature phosphorescence detection of enoxacin in biological fluids, Anal. Chem., 80 (2008) 3832–3837.
[35] W.S. Zou, D. Sheng, X. Ge, J.-Q. Qiao, H.-Z. Lian, Room-temperature phosphorescence chemosensor and rayleigh scattering chemodosimeter dual-recognition probe for 2,4,6-trinitrotoluene based on manganese-doped ZnS quantum dots, Anal. Chem., 83 (2011) 30–37.
[36] M.E. Pacheco, C.B. Castells, L. Bruzzone, Mn-doped ZnS phosphorescent quantum dots: coumarins optical sensors, Sens. Actuators, B, 238 (2017) 660–666.
[37] P. Deng, L. Lu, T. Tan, Y. Jin, X. Fan, W. Cao, X. Tian, Novel phosphorescent Mn-doped ZnS quantum dots as a probe for the detection of L-tyrosine in human urine, Anal. Methods, 9 (2017) 287–293.
[38] J.S. Pinter, K.L. Brown, P.A.D. Young, G.F. Peaslee, Amperometric detection of hydrazine by cyclivoltammetry and flow injection analysis using ruthenium modified glassy carbon electrodes, Talanta, 71 (2007) 1219–1225.
[39] L. Zheng, J. Song, Curcumin multi-wall carbon nanotubes modified glassy carbon electrode and its electrocatalytic activity towards oxidation of hydrazine, Sens. Actuators, B, 135 (2009) 650–655.
[40] G. Wang, C. Zhang, X. He, Z. Li, X. Zhang, L. Wang, B. Fang, Detection of hydrazine based on nano-Au deposited on porous-TiO_2 film, Electrochim. Acta, 55 (2010) 7204–7210.
[41] N. Maleki, A. Safavi, E. Farjami, F. Tajabadi, Palladium nanoparticle decorated carbon ionic liquid electrode for highly efficient electrocatalytic oxidation and determination of hydrazine, Anal. Chim. Acta, 611 (2008) 151–155.
[42] C.C. Yang, A.S. Kumar, M.C. Kuo, S.H. Chien, J.M. Zen, Copper–palladium alloy nanoparticle plated electrodes for the electrocatalytic determination of hydrazine, Anal. Chim. Acta, 554 (2005) 66–73.
[43] H. Zhang, J. Huang, H. Hou, T. You, Electrochemical detection of hydrazine based on electrospun palladium nanoparticle/carbon nanofibers, Electroanalysis, 21 (2009) 1869–1872.
[44] C. Bathchelor-McAuley, C.E. Banks, A.O. Simm, T.G.J. Jones, R.G. Compton, The electroanalytical detection of hydrazine: a comparison of the use of palladium nanoparticles supported on boron-doped diamond and palladium plated BDD microdisc array, Analyst, 131 (2006) 106–110.
[45] X. Ji, C.E. Banks, A.F. Holloway, K. Jurkschat, C.A. Thorogood, G.G. Wildgoose, R.G. Compton, Palladium sub-nanoparticle decorated 'bamboo' multi-walled carbon nanotubes exhibit electrochemical metastability: voltammetric sensing in otherwise inaccessible pH ranges, Electroanalysis, 18 (2006) 2481–2485.
[46] M. Faisal, Md.A. Rashed, M.M. Abdullah, F.A. Harraz, M. Jalalah, M.S. Al-Assiri, Efficient hydrazine electrochemical sensor based on PANI doped mesoporous $SrTiO_3$ nanocomposite modified glassy carbon electrode, J. Electroanal. Chem., 879 (2020) 114805, doi: 10.1016/j.jelechem.2020.114805.
[47] A. Mejri, A. Mars, H. Elfil, A.H. Hamzaoui, Curcumin graphite pencil electrode modified with molybdenum disulfide nanosheets decorated gold foams for simultaneous quantification of nitrite and hydrazine in water samples, Anal. Chim. Acta, 1137 (2020) 19–27.

[48] S. Antherjanam, B. Saraswathyamma, Simultaneous electrochemical determination of hydrazine and hydroxylamine on a thiadiazole derivative modified pencil graphite electrode, Mater. Chem. Phys., 275 (2022) 125223, doi: 10.1016/j.matchemphys.2021.125223.

[49] Y. Jia, N. Shang, X. He, A. Nsabimana, Y. Gao, J. Ju, X. Yang, Y. Zhang, Electrocatalytically active cuprous oxide nanocubes anchored onto macroporous carbon composite for hydrazine detection, J. Colloid Interface Sci., 606 (2022) 1239–1248.